Organic Process Research & Development **2006**, *10*, 727−732

Constant Supersaturation Control of Antisolvent-Addition Batch Crystallization

Nobuaki Nonoyama,* Keigo Hanaki, and Yasuaki Yabuki

Process Research, Banyu Pharmaceutical Co., Ltd., 3-9-1 Kamimutsuna, Okazaki, Aichi 444-0858, Japan

Abstract:

We have developed a simple method to design antisolvent-addition crystallization by using a numerical simulation. To design the reasonable conditions, e.g. the profile of antisolvent addition, seed loading, and minimum time cycle, a numerical simulation was applied using kinetic parameters obtained from experiments. ReactIR was used for on-line monitoring, which enabled the concentration, supersaturation, and growth rate to be monitored throughout the crystallization process. This model takes into account only growth and ignores nucleation, agglomeration, and breakage. The results of the numerical simulations agreed well with the corresponding experimental results and assisted in the design of a suitable crystallization process.

1. Introduction

Antisolvent-addition batch crystallization, sometimes referred to as dilution crystallization, is commonly used for the small-scale production of fine chemicals, active pharmaceutical ingredients (API), and their intermediates. Robustness and accurate quality control are required to manufacture these compounds. Especially in the production of final API crystals, the quality requirements with regard to purity, size distribution, and crystal form are very high. We are working on APIs in the preclinical development stage where we often need to develop and scale up crystallization processes in a short period of time for on-time bulk supply and for larger-scale manufacturing. Therefore, an easy and quick procedure to develop a robust and proper crystallization process is needed.

The crystallization process for the compound of interest had several key objectives, such as impurity rejection and polymorph control. Of these issues, polymorph control was the primary driving force in this study, since the solubility of one undesired polymorph was only 10−20% higher than that of the desired polymorph. For this compound, introduction of the undesired polymorph must be avoided. Therefore, an initial goal was to keep the supersaturation below a certain level throughout the process to avoid nucleation of the undesired polymorph.

Although crystallization is a common subject of investigation, considerable experimental trial and error is still needed to develop a robust process due to the complexity and variety of crystallization behaviors displayed by organic compounds. Crystallization processes are influenced by the following factors; solubility, supersaturation, seed loading, crystal shape factor, agitation, growth rate kinetics, nucleation rate kinetics, agglomeration kinetics, etc.[1] Incorporation of all possible factors into a model can lead to the need to estimate many parameters. In practice, it is convenient to describe a crystallization process using as few parameters as possible while retaining a reasonable degree of model accuracy. Our purpose is to develop a simple numerical simulation of crystallization to understand and design a crystallization process with practical accuracy.

There have been only a few reports on antisolvent-addition crystallization[2−5] Tavare (1995) briefly described an optimal antisolvent-addition profile.[6] Otherwise, there have been no reports on general optimization methodologies. He treated antisolvent-addition crystallization in a similar manner as cooling crystallization, and obtained an antisolvent concentration curve by maintaining a constant supersaturation, as described in eq 1:

$$\frac{U - U_{\text{initial}}}{U_{\text{final}} - U_{\text{inital}}} = \left(\frac{t}{t_{\text{final}}}\right)^4 \tag{1}$$

This curve was derived under the following assumptions: no seed, linear solubility relation, and simple power-law growth and a nucleation rate that is independent of the solution composition. Unfortunately, these assumptions are not in agreement with our compound of interest, for which the growth rate is a strong function of solvent composition and the solubility is not linear. Therefore, we cannot use this curve for our compound.

In this, we describe a sequence of experiments and a simple numerical simulation that predicts the experimental results, and we also calculate the ideal antisolvent-addition profile. Through the recent development of an in situ monitoring technique,[7−9] it has become easier to obtain

* Author for correspondence. Process Research, Banyu Pharmaceutical Co., Ltd., 3-9-1 Kamimutsuna, Okazaki, Aichi 444-0858, Japan. Telephone: +81-564-51-5668; Fax: +81-564-51-7086; E-mail: nobuaki_nonoyama@merck.com.

(1) Mullin, J. W. *Crystallization*, 4th ed.; Butterworth-Heinemann: London, 2001.
(2) Gabas, N.; Laguérie, C. Batch Crystallization of D-Xylose by Programmed Cooling or by Programmed Adding of Ethanol. *Chem. Eng. Sci.* **1992**, *47*, 3148.
(3) Doki, N.; Kubota, N.; Yokota, M.; Kimura, S.; Sasaki, S. Production of Sodium Chloride Crystals of Unimodal Size Distribution by Batch Dilution Crystallization. *J. Chem. Eng. Jpn.* **2002**, *35*, 1099−1104.
(4) Holmbäck, X.; Rasmuson, Å. C. Size and Morphology of Benzoic Acid Crystals Produced by Drowning-out Crystallization. *J. Cryst. Growth* **1999**, *198/199*, 780−788.
(5) Kaneko, S.; Yamagami, Y.; Tochihara, H.; Hirasawa, I. Effect of Supersaturation on Crystal Size and Number of Crystals Produced in Antisolvent Crystallization. *J. Chem. Eng. Jpn.* **2002**, *35*, 1219−1223.
(6) Tavare, N. S. *Industrial Crystallization*: Plenum Press: New York, 1995, 112−118.
(7) Lewiner, F.; Klein, J. P.; Puel, F.; Fevotte, G. On-line ATR FTIR Measurement of Supersaturation During Solution Crystallization Processes. Calibration and Applications on Three Solvent/Solute Systems. *Chem. Eng. Sci.* **2001**, *56*, 2069−2084.

10.1021/op0600052 CCC: $33.50
Published on Web 05/19/2006

kinetic data. We can quickly and reliably design a reasonable crystallization process with minimal experiments using on-line monitoring tools. This method can be applied to the antisolvent-addition batch crystallization of a wide range of compounds.

2. Modeling

The model is based on basic crystallization equations. From a practical perspective, to maintain a reasonable degree of accuracy, the model was simplified by making the following assumptions:

- size-independent crystal growth
- no nucleation
- no agglomeration
- no breakage
- self-symmetrical crystal growth
- uniformity within the vessel

2.1. Liquid Phase. Concentration (C) and solubility (C_s) are shown in units of [g/g(total solvent weight W)], which simplify the calculation since there is no need to know volume or density. The dissolved solute weight (M) is thus the product of concentration (C) and total solvent weight (W).

$$M = WC \tag{2}$$

The solubility is expressed as a function of solvent composition (Q) at a constant temperature.

$$\mathbf{Q} = \frac{\text{weight of water}}{\text{total solvent weight}} \tag{3}$$

$$C_s = C_s(\mathbf{Q},T) \tag{4}$$

The rate of solute decrease, equal to the crystal growth rate, is proportional to the crystal surface area (A) and the driving force of supersaturation (ΔC), where the crystal growth constant (k_g) is a function of solvent composition (Q), temperature, agitation, size, etc. In this study, all experiments were carried out at the same temperature and agitation speed, and by assuming size-independent growth, we considered k_g to be a function of only the solvent composition (Q).

$$\frac{dM}{dt} = -k_g A \Delta C \tag{5}$$

$$k_g = k_g(\mathbf{Q},T,\text{agitation,size,...}) \tag{6}$$

We used eq 7 for the driving force (ΔC) for crystallization, as suggested by Mohan and Myerson from a thermodynamic perspective and in combination with the Burton−Cabrera−Frank crystal growth model.[10]

$$\Delta C = (\ln(C/C_s))^2 \tag{7}$$

$$\Delta C = (C - C_s)^g \tag{8}$$

Equation 8 presents the well-known power law form; however, it was not suitable for this study. When eq 8 is used instead of eq 7, there is so much variation in $(C - C_s)^g$ with changes in C and C_s over a wide range that the value of k_g is unstably dispersed.

2.2. Solid Phase. The weight of crystal (P) can be calculated from the initial solid weight (P_0, equal to the seed amount), the initial solute amount (M_0), and the dissolved solute (M)

$$P = P_0 + M_0 - M \tag{9}$$

The surface area of the crystal is expressed as eq 10, based on the assumption of self-symmetrical crystal growth.

$$A = A_0\left(\frac{P}{P_0}\right)^{2/3} \tag{10}$$

2.3. Simulation Algorithm. We made a simulation program based on the above model. Given the initial conditions P_0 and M_0, and a solvent composition profile as a function of time ($Q(t)$), this program can be used to predict the concentration (C), supersaturation ($(C - C_s)/C_s$), and growth rate (dM/dt). The simulation program consists of simple step-forward calculation. At each moment, the change in solute weight (ΔM) over a small-increment time-step (Δt) can be calculated from eq 11, in which all values are derived from eqs 2−4, 6, 7, 9, and 10.

$$\Delta M = -k_g A \Delta C \cdot \Delta t \tag{11}$$

$$M(t + \Delta t) = M(t) + \Delta M \tag{12}$$

The program calculates repeatedly until the end and gives the profiles of C, supersaturation, and dM/dt throughout the process.

3. Experimental Section

Typical Crystallization Procedure. Crystallizations were carried out in a 1-L jacketed glass vessel equipped with ReactIR (Mettler-Toledo K.K.), FBRM (Mettler-Toledo K.K.), a thermocouple, and an overhead blade stirrer. Compound P (50 g) was dissolved in solvent (410 g) and heated to 60 °C. The solution was cooled to 50 °C, resulting in a ca. 15% supersaturation solution. Seed (1.0 g, 2 wt %, surface area = 3.0 m^2/g), was introduced and the mixture was stirred for 30 min. Water (200 g) was added as an antisolvent for several hours at a controlled rate, as described in the next section. The temperature and stirring speed were kept constant at 50 °C and 500 rpm throughout the process. The slurry was filtered and washed with water (100 g × 2). The cake was blown with N_2 and dried overnight under vacuum at 50 °C. Particle sizes were analyzed with MICROTRAC (model 9320-X100). Crystal forms were analyzed with X-ray powder diffraction (X'Pert PRO MPD), and the peaks of undesired form were not detected in all experiments.

(8) Togkalidou, T.; Tung, H.-H.; Sun, Y.; Andrews, A.; Braatz, R. D. Solution Concentration Prediction for Pharmaceutical Crystallization Processes Using Robust Chemometrics and ATR FTIR Spectroscopy. *Org. Process Res. Dev.* **2002**, *6*, 317−322.

(9) Yu, L. X.; Lionberger, R. A.; Raw, A. S.; D'Costa, R.; Wu, H.; Hussain, A. S. Applications of Process Analytical Technology to Crystallization Processes. *Adv. Drug Delivery Rev.* **2004**, *56*, 349−369.

(10) Mohan, R.; Myerson, A. S. Growth Kinetics: A Thermodynamic Approach. *Chem. Eng. Sci.* **2002**, *57*, 4277−4285.

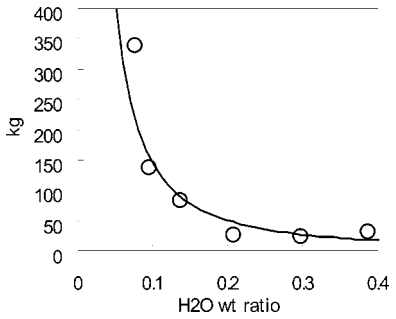

Figure 1. **Growth rate constants (k_g) obtained from an antisolvent spiking addition experiment and power curve fitting.**

The batch was monitored by ReactIR and FBRM every two minutes. Small aliquots were also sampled intermittently for HPLC analysis. IR absorbance data were processed, second-derivatives were taken, and smoothing was applied, and the results were calibrated with concentration data obtained from HPLC. One of the peaks that showed a nice linear relation to the concentration was used to convert IR absorbance to concentration. Please see Supporting Information for detailed data processing.

4. Results and Discussion

4.1. Introduction. Compound P is a typical pharmaceutical organic compound with a molecular weight of ca. 400 and both aromatic and heteroaromatic rings. It dissolves well in polar organic solvents and scarcely dissolves in water. Thus, in this study, the compound was first dissolved in polar organic solvent, and then water was added as an antisolvent.

Some of the physical properties of compound P need to be obtained from experiments for the model calculation. Agglomeration and nucleation were neglected in this study, and thus only the growth rate constant (k_g) and solubility (C_s) are required. First, we measured C_s and outlined the crystallization process: start, seeding, and end points (section 4.2.). Next, throughout the entire crystallization process, k_g was obtained from an antisolvent spiking addition experiment (4.3). Using the obtained physical properties, simulations were carried out under various conditions, and the results were compared with the corresponding experimental results (4.4). In addition, the ideal antisolvent-addition profile to maintain a constant supersaturation was calculated based on the same model, and minimal time cycles were estimated under several conditions (4.5).

4.2. Solubility Measurement and Outline of the Process. Excess compound P was placed in a series of vials of various solvent compositions. The resulting vials were stirred overnight at 50 °C and the supernatants were analyzed by HPLC. The results are shown in Figure 1. A fourth-polynomial curve was fitted to the experimental points and the correlation between C_s and Q was obtained.

$$C_s(Q) = 8.0004Q^4 - 12.1640Q^3 + 7.1961Q^2 + 1.9982Q + 0.2251 \quad (13)$$

From the solubility curve, we chose the start and end points at $Q = 0.08$ and 0.35, respectively, where the solubility decreases from 0.107 to 0.004 g/g. To achieve moderate supersaturation at the seed point, the initial concentration of compound P was set at 0.122 g/g.

4.3. Antisolvent Spiking Addition Experiment To Obtain k_g. To obtain k_g throughout the entire process, antisolvent spiking addition experiments were carried out. Some amount of water was added in one minute to attain 15−30% supersaturation. The de-supersaturation curve was then monitored for a couple of hours. This procedure was repeated at several points over the entire range of solvent composition. From each de-supersaturation curve, k_g at each solvent composition was calculated based on eq 5 (Figure 1.). The results were fitted to a power function curve to give an equation for k_g as a function of Q (eq 14). This relation was used for the following simulations.

$$k_g(Q) = 4.23Q^{-1.54} \quad (14)$$

4.4. Continuous Antisolvent-Addition Experiments. To verify the simulation program, three experiments with different antisolvent addition profiles were carried out. The concentration was monitored with ReactIR, and the results were compared to the corresponding simulation output. In all three experiments, no significant nucleation was observed on FBRM, and crystals seemed to grow smoothly. The three experiments had the same initial and final conditions as described above, i.e. the same amounts of solvent (410 g), compound P (50 g), and seed (1.0 g) were used, and the same amount of antisolvent (200 g) was then added at different rates.

Case 1: Addition over 3 h in One Step. To a supersaturated solution, seed (1.0 g) was added, and the mixture was stirred for 30 min. Antisolvent (200 g) was then added at a constant rate for 3 h. The experimental results are shown in Figure 2. Supersaturation exceeded 30% in the early stage due to a sharp drop in solubility at a low water composition. The dashed line in Figure 2 shows the output of the simulation. The results agree nicely with the experimental results. Thus, from the initial conditions and the antisolvent-addition profile, the simulation program could accurately predict the experimental results.

Case 2: Addition over 3 h in Three Steps. The initial conditions and seeding were the same as in case 1, but antisolvent was added in three phases at different rates over a total of 3 h. The rate of addition was initially slow (30 g/h) and then increased (60 and 110 g/h). The experimental results are shown in Figure 3. Supersaturation was kept constant at about 20% throughout the addition of antisolvent. The corresponding simulation results (dashed line in Figure 3) agreed well with the experimental results. With the slow addition of antisolvent at the initial stage, solubility drops moderately, and thus the rapid increase to a high supersaturation, as observed in case 1, is avoided. Although the same amount of antisolvent was added over the same time period as in case 1, supersaturation remained low in case 2. In case 2, the possibility of nucleation is lower than in case 1 for a lower supersaturation. Accordingly, the profile for case 2 is preferable to that of case 1 for avoiding nucleation.

Case 3: Addition over 5 h in Five Steps. The initial conditions and seeding in case 3 were again the same as in

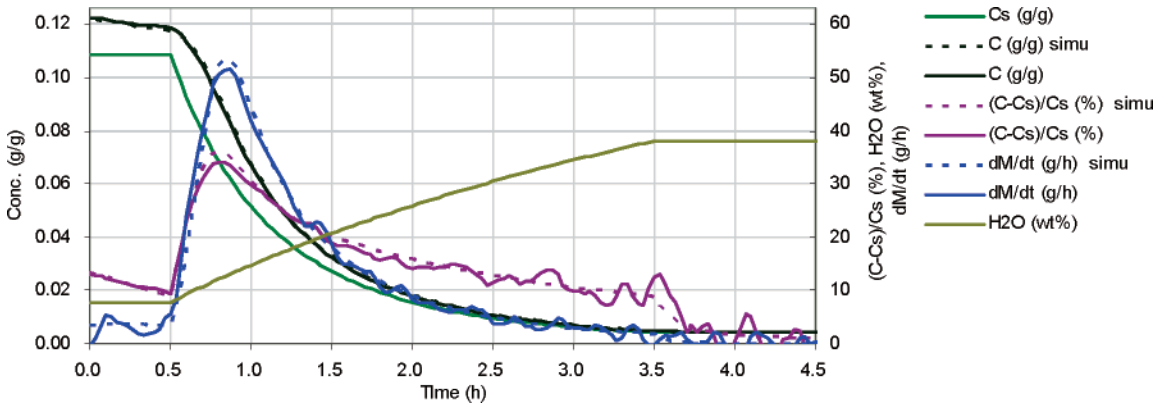

Figure 2. **Experimental and simulation results for case 1.**

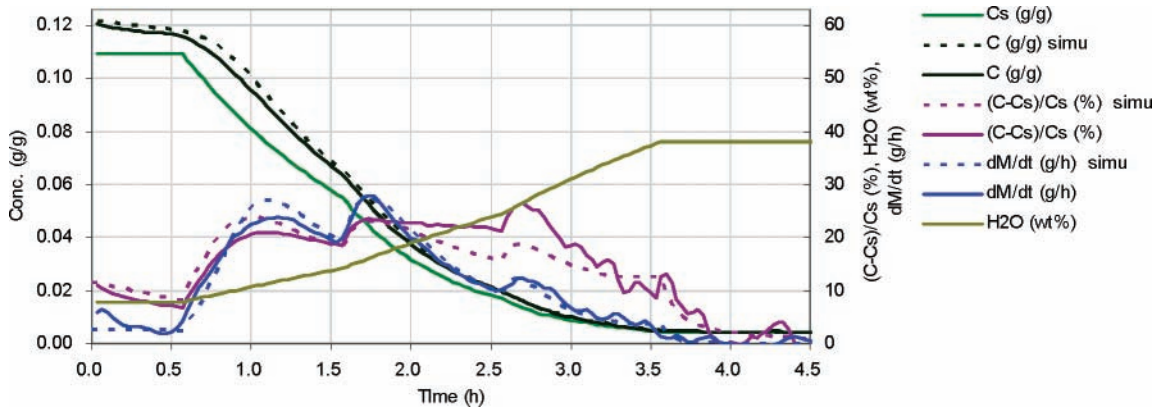

Figure 3. **Experimental and simulation results for case 2.**

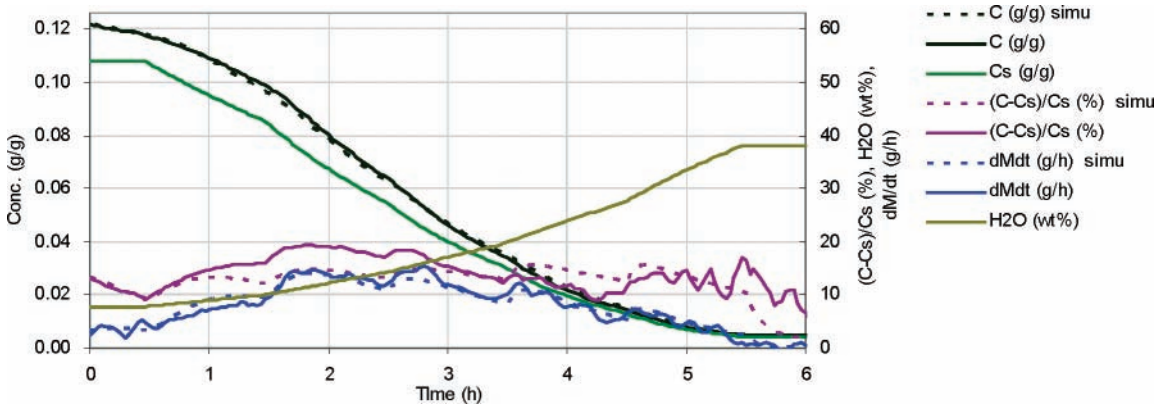

Figure 4. **Experimental and simulation results for case 3.**

cases 1 and 2. Antisolvent was added in five phases at different rates over a total of 5 h. Addition was started at a slow rate and then gradually accelerated (10, 20, 30, 50, and 90 g/h). The total amount of antisolvent added was the same as in cases 1 and 2, but the addition occurred over a longer period. The experimental results are shown in Figure 4. The simulation results (dashed line in Figure 4) roughly correspond to the experimental results. Supersaturation was kept constant at about 15% throughout the addition of antisolvent. With the initial very slow addition and longer addition period, the supersaturation profile was preferable to those in cases 1 and 2 with respect to the avoidance of nucleation.

As described in the above three cases, the experimental and simulation results showed good agreement. The signal-noise ratio of IR signal at low substance concentration range is relatively large, therefore, the error of substance concentration seems large in the later stage of each case. Although the effects were not observed in these three cases, above a certain level of supersaturation, nucleation and agglomeration cannot be ignored and may deteriorate the accuracy of the simulation. While this is certainly a limitation of this model, we would try to avoid such a high supersaturation in our crystallization process to minimize nucleation. Thus, this simulation is not intended to be used under such conditions.

Particle size data obtained with MICROTRAC and FBRM at the final stage of each experiment are shown in Table 1. Assuming neither nucleation nor aggregation, the calculated value of ideal growth from 4 μm seed crystals was 14.7 μm. The mean values of the resulting PSDs in cases 1−3 were

Table 1. **Particle size information**

	MICROTRAC [a]			FBRM chord length	
	mean (μm)	d95% (μm)	SD (μm)	no weight mean (μm)	length wt mean (μm)
seed	4	8	2		
case 1	16	32	9	23.9	39.9
case 2	17	36	10	21.8	36.6
case 3	16	35	10	20.3	34.4
model	14.7				

[a] Dispersed with sonication

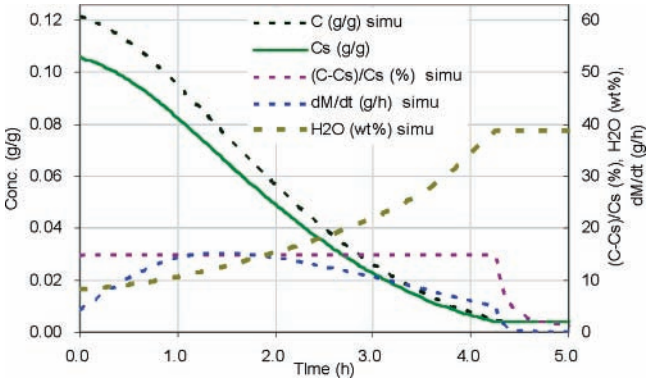

Figure 5. **Calculated ideal antisolvent-addition profile to maintain supersaturation at 15%.**

close to that of the ideal growth model, which suggests that there was no significant nucleation in these experiments.

4.5. Calculation of Antisolvent-Addition Profile To Maintain a Constant Supersaturation. Procedures for the crystallization of API compounds are usually required to reproducibly yield uniform-quality crystals in a minimal time cycle, i.e., contamination by undesired polymorphs must be avoided, and they should always give a similar particle-size distribution. To achieve these characteristics, nucleation should be avoided. If a compound has polymorphs, the nucleation of some forms may occur above a certain level of supersaturation, and crystals contaminated with the undesired polymorphs may be obtained. When nucleation occurs, the particle-size distribution becomes irregular and is difficult to control.

To avoid nucleation, supersaturation should be kept in the metastable zone throughout the process. However, it is usually very difficult to find the metastable zone for secondary nucleation. While a very low supersaturation can be used to avoid nucleation, it can be very time-consuming and impractical. Accordingly, it is reasonable to maintain moderate supersaturation throughout the process to avoid nucleation and minimize the time required for the process.

The present model was used to calculate the rate of antisolvent addition to maintain a constant supersaturation. Given the initial conditions, C_s is calculated under the restriction that supersaturation $((C - C_s)/C_s)$ is constant. Next, Q is calculated from a polynomial function of $C_s(Q)$. The subsequent sequence is the same as that described in section 2.3. Thus, we obtain a concentration profile ($C(t)$) and an antisolvent-addition profile ($Q(t)$). Figure 5 shows the results of the calculation when the supersaturation was kept constant at 15% under the same initial conditions as in the above three experiments (section 4.4). At the beginning of the process, the solubility curve in the region of low water content is steep, and the crystals have a small surface area. Therefore, the program indicated that the antisolvent should be added very slowly to gradually decrease the batch solubility. In a later stage, the solubility curve with higher water content is flatter and the surface area is greater, and thus antisolvent can be added more rapidly. If the process follows this antisolvent-addition profile, supersaturation will be kept constant at 15%, and hence it shows a minimal batch time cycle under this restriction and the initial conditions. In practice, the addition curve can be approximated by several steps of linear addition, as in case 3 in section 4.4.

Table 2. **Estimation of the batch cycle time under various conditions**

entry	seed (wt %)	supersaturation (%)	time (h)
1	2	15	4.3
2	4	15	3.2
3	6	15	2.7
4	4	10	6.5
5	4	20	2.0

Antisolvent-addition profiles were calculated under various conditions (Table 2). While the initial amounts of solvent and solute were the same as in the above experiments, the amount of seed and supersaturation were altered. The seed is assumed to have the same surface area per gram as the seed used in the above experiments. Entries 1−3 in Table 2 compare differences in the amount of seed at the same supersaturation level. The duration of antisolvent addition is reduced with an increase in the amount of seed. Entries 2, 4, and 5 show the antisolvent-addition time with varying allowance of supersaturation. When supersaturation is limited to 10%, antisolvent addition takes 6.5 h, whereas in the case of 20% supersaturation, it takes only 2 h. If the metastable zone is wide and no nucleation occurs, the use of a high supersaturation can shorten the process cycle time.

5. Conclusion

The antisolvent-addition crystallization of API was studied by using a simple simulation program. This process was designed to avoid nucleation by keeping supersaturation below a certain level. This process was successfully scaled up to a pilot-plant scale and gave more than 100 kg of API crystals. In pilot-plant production, an antisolvent-addition procedure was designed to keep supersaturation under 10% to minimize the risk of generating wrong polymorphs which have only 10−20% higher solubility under these experimental conditions. As a result, crystals of the desired form were obtained exclusively, and similar particle-size distributions were obtained reproducibly.

As described above, a rapid procedure for the constant supersaturation control of antisolvent-addition crystallization was established. In conventional process development, many experiments are needed to identify a good process, which may not be optimal. In this study, by measuring the growth rate constant and solubility curve in just a few experiments,

we obtained an ideal antisolvent-addition profile by using a simulation. We were also able to estimate the batch cycle time under arbitrary conditions. This procedure can be easily applied to develop a crystallization process for a wide variety of compounds.

Notations

GLOSSARY

A	total surface area of crystal (m^2)
A_0	surface area of seed crystal (m^2)
C	concentration (g/g(solvent))
C_s	solubility (g/g(solvent))
g	growth rate order
k_g	growth rate coefficient (g/h)
M	weight of compound P dissolved in solution (g)
Q	weight fraction of antisolvent
W	weight of solution (g)
P	weight of compound P in the solid phase (g)
P_0	weight of seed (g)
T	temperature
U	antisolvent concentration
subscript 0	initial condition

Acknowledgment

The authors thank Miwako Asada for analytical assistance. We also thank Hsien-Hsin Tung and Zhihao Lin for helpful discussions.

Supporting Information Available

The detailed procedure of data processing from IR data to substance concentration. This material is available free of charge via the Internet at http://pubs.acs.org.

Received for review January 4, 2006.

OP0600052